Monthly Notices of the ROYAL ASTRONOMICAL SOCIETY

MNRAS **436,** 395–400 (2013) doi:10.1093/mnras/stt1572
Advance Access publication 2013 September 11

Detection of Hα emission from $z > 3.5$ submillimetre luminous galaxies with *AKARI*-FUHYU spectroscopy

Chris Sedgwick,[1⋆] Stephen Serjeant,[1] Chris Pearson,[1,2] Ian Smail,[3] Myungshin Im,[4] Shinki Oyabu,[5] Toshinobu Takagi,[6] Hideo Matsuhara,[6] Takehiko Wada,[6] Hyung Mok Lee,[4] Woong-Seob Jeong[7] and Glenn J. White[1,2]

[1] *Department of Physical Sciences, The Open University, Milton Keynes MK7 6AA, UK*
[2] *RAL Space, Rutherford Appleton Laboratory, Chilton, Didcot, Oxfordshire OX11 0QX, UK*
[3] *Institute for Computational Cosmology, Durham University, Durham DH1 3LE, UK*
[4] *Department of Physics and Astronomy, Seoul National University, Seoul 151-742, Korea*
[5] *Graduate School of Science, Nagoya University, Furo-cho, Chikusa-ku, Nagoya, Aichi 464-8602, Japan*
[6] *Institute of Space and Astronautical Science, Japan Aerospace Exploration Agency, Sagamihara, Kanagawa 229 8510, Japan*
[7] *Korea Astronomy & Space Science Institute, 776 Daedeok-daero, Yuseong-gu, Daejeon 305-348, Korea*

Accepted 2013 August 20. Received 2013 August 19; in original form 2012 November 14

ABSTRACT

We present tentative Hα emission line detections of four submillimetre-detected galaxies at $z > 3.5$: the radio galaxies 8C1909+722 and 4C60.07 at signal-to-noise ratios (SNRs) of 3.1 and 2.5, and two submillimetre-selected galaxies (SMGs) near the first of these at SNRs of 10.0 and 2.4, made with the *AKARI* space telescope as part of the Follow-Up Hayai-Yasui-Umai mission programme. These are the highest redshift Hα detections in such galaxies, made possible by *AKARI*'s unique near-infrared spectroscopic capability. The two radio galaxies had known redshifts and surrounding structure, and we have detected broad Hα components indicating the presence of dust-shrouded quasars. We conclude that powerful active galactic nuclei (AGNs) at $z > 3.5$ occur in peaks of the star formation density fields, supporting a close connection between stellar mass build-up and black hole mass assembly at this redshift. We also show that 4C60.07 is a binary AGN. The Hα detections of the two SMGs are the first redshift determinations for these sources, confirming their physical association around their companion radio galaxy. The Hα-derived star formation rates (SFRs) for the SMGs are lower than their far-infrared derived SFRs by a factor of ∼10, suggesting a level of dust obscuration similar to that found in studies at $\sim 1 < z < 2.7$.

Key words: galaxies: active – galaxies: evolution – galaxies: starburst – galaxies: star formation – infrared: galaxies.

1 INTRODUCTION

The interaction between active galactic nuclei (AGNs) and star formation in galaxies is a key question in cosmology. For local galaxies, Magorrian et al. (1998) found a relation between black hole mass and stellar bulge mass, and Ferrarese & Merritt (2000) and Gebhardt et al. (2000) found a tight correlation between black hole mass and stellar velocity dispersion, so it is widely accepted that the two are intimately related. The redshift evolution of the cosmic star formation rate (SFR) is remarkably similar to that of quasar luminosity density (Boyle & Terlevich 1998; Chapman et al. 2005) and black hole accretion (Franceschini et al. 1999). Mid-infrared spectroscopy has shown that most ultra-luminous infrared galaxies (ULIRGs, $10^{12}\,L_\odot < L_{IR} < 10^{13}\,L_\odot$) have simultaneous AGN and starburst activity in their nuclei (Genzel et al. 1998; Spoon et al. 2007).

Various models have been developed to explain the dynamics underlying these observations. Simulations of galaxy mergers have incorporated the growth of black holes and star formation, showing AGN feedback as a mechanism to regulate SFR (e.g. di Matteo et al. 2005; Springel, Di Matteo & Hernquist 2005). Semi-analytic source count models can best reproduce massive galaxy number densities when incorporating AGN feedback in the coevolution of galaxies and their central black holes (e.g. Bower et al. 2006; Croton et al. 2006).

Observational constraints for such models from high-redshift galaxies are now becoming available. Studies using a combination of submillimetre and X-ray observations at $z \sim 2$ have confirmed the association of AGNs and intense star formation (Alexander et al. 2005; Harrison et al. 2012).

The discovery of high-redshift submillimetre galaxies (Smail, Ivison & Blain 1997; Barger et al. 1998; Hughes et al. 1998) and their possible association with high-redshift radio galaxies (HzRGs;

⋆ E-mail: chris@bbsbafca.demon.co.uk

Published by Oxford University Press on behalf of the Royal Astronomical Society

Table 1. Sample of high-redshift radio galaxies and submillimeter-selected sources. The 850 μm flux data from SCUBA and the target coordinates are from Stevens et al. (2003).

Source	RA (J2000)	Dec. (J2000)	Redshift (z)	850 μm flux (mJy)	*AKARI* NIR Spectroscopy Observation ID	Dates	Exposure (min)
8C1909+722 HzRG	19 08 23.3	+72 20 10.4	3.536 ± 0.0003	34.9 ± 3.0	1370153	8/2008(1), 8/2009(9)	93
SMMJ190827+721928 (SMM1)	19 08 27.4	+72 19 28.0	–	23.0 ± 2.5	1370154	8/2008(10)	93
SMMJ190829+722050 (SMM2)	19 08 29.3	+72 20 49.6	–	8.7 ± 2.4	1370155	8/2009(10)	93
SMMJ190816+722024 (SMM3)	19 08 16.1	+72 20 24.0	–	4.3 ± 2.1	1370156	8/2008(5), 2/2009(2), 8/2009(3), 2/2010(3)	120
4C60.07 HzRG	05 12 54.8	+60 30 51.7	3.788 ± 0.004	23.8 ± 3.5	1370162	6/2008(9), 6/2009(1)	93

e.g. Stevens et al. 2003) implies that there are regions of intense star formation which also show strong radio emission at high redshift. Detection of emission lines from these galaxies in the infrared can be used to confirm this connection and to provide an independent measure of SFRs and AGN activity.

Spectroscopy of HzRGs and submillimetre galaxies has previously been made in the near-infrared (NIR) K band (Swinbank et al. 2004). The *AKARI* space telescope (Murakami et al. 2007) could obtain spectra at longer NIR wavelengths between 2.5 and 5.0 μm, a region not previously available for spectroscopy by other infrared space missions such as *Spitzer* space telescope (and with poor sensitivity from the ground), giving the possibility of detecting Hα for galaxies at $3.0 < z < 6.5$.

This paper presents tentative Hα detections from *AKARI* observations of HzRGs and submillimetre galaxies. Data collection and reduction are discussed in Section 2. Results are presented in Section 3 and discussed in Section 4. We assume $H_0 = 72.0\,\mathrm{km\,s^{-1}\,Mpc^{-1}}$, $\Omega_M = 0.3$ and $\Omega_\Lambda = 0.7$.

2 DATA COLLECTION AND REDUCTION

2.1 *AKARI*-FUHYU mission programme

The *AKARI* 'Follow-Up Hayai-Yasui-Umai' mission programme (FUHYU; Pearson et al. 2010) used the *AKARI* Infrared Camera (IRC; Onaka et al. 2007) to carry out imaging and spectroscopy of well-studied galaxies rich in multiwavelength data, often with known redshifts, to maximize the legacy value of the *AKARI* data. The mission programme carried out extensive infrared imaging during the first two phases of the *AKARI* mission; the NIR spectroscopic campaign was carried out during Phase III, the warm phase after cryogen exhaustion. Spectroscopy was carried out using the IRC grism over a 1 arcmin × 1 arcmin point source aperture centred on 46 submillimetre and radio galaxies from 2008 June–2010 May. We will be reporting later on results for the rest of our FUHYU mission programme targets.

2.2 Targets Observed

Observations were made of two HzRGs and three submillimetre sources potentially associated with one of them (see Table 1 and Fig. 1). Stevens et al. (2003) described submillimetre mapping of these radio sources by the Submillimeter Common-User Bolometer Array (SCUBA) instrument on the James Clerk Maxwell Telescope and suggested that the submillimetre sources observed were associated with the nearby radio source on the basis of their number densities and positions relative to the radio jets.

8C1909+722 and companions. The redshift was reported in De Breuck et al. (2001) based on a deep Keck optical spectrum showing strong Lyα emission with full width at half-maximum (FWHM) = 1200 ± 90 km s^{-1}. This field was included in an 850 μm survey of the environments of HzRGs which detected three nearby submillimetre galaxies (Stevens et al. 2003). Two of the three submillimetre sources (SMM1 and SMM2) were later detected at 350 μm with SHARC-II on the Caltech Submillimeter Observatory

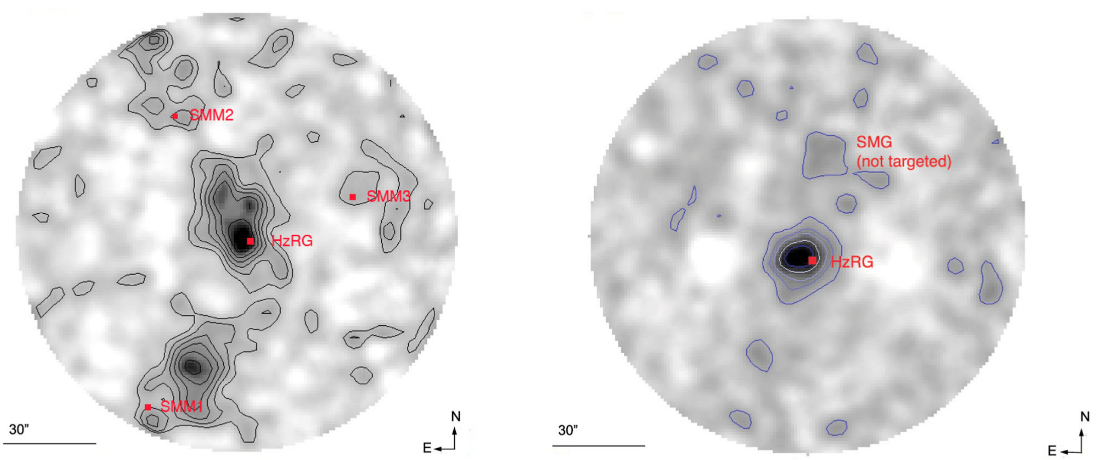

Figure 1. Left: SCUBA 850 μm image and contours (at 0.5, 1, 1.5, 2, 2.5 and 3 σ) for 8C1909+722 with the positions of the four *AKARI* spectra marked in red. Right: SCUBA 850 μm image and contours (at 1, 2, 3 and 4 σ) for 4C 60.07 with the position of the *AKARI* spectrum marked in red. This does not resolve the sources within the central contour (see Fig. 3 for SMA 870 μm contours). The SCUBA maps are from Stevens et al. (2003).

(Greve, Ivison & Stevens 2006). A recent study using JVLA and IRAM PdBI radio observations and *Herschel* data at 100–500 μm (Ivison et al. 2012) found a large red dust feature aligned with the radio jet and SMM1, and it concluded that SMM1 probably shared the same node or filament of the cosmic web as the radio galaxy, although it did not detect convincing ^{12}CO emission from SMM1. Redshifts for these submillimetre-selected galaxies (SMGs) were not previously known.

4C60.07. The redshift for this galaxy is based on the Lyα emission line (Roettgering et al. 1997) with FWHM = 2880 ± 940 km s^{-1}. Dust emission was detected at 850 μm and 1.25 mm (Papadopoulos et al. 2000), and CO $J = 1$–0 emission (Greve, Ivison & Papadopoulos 2004). A detailed SMA, *Spitzer* and Very Large Array study by Ivison et al. (2008) suggested an early-stage merger between the host galaxy of an AGN (the HzRG) and a companion starburst/AGN (which they labelled 'B'; see Fig. 3). They proposed that a second submillimetre source, which they labelled 'A', although of roughly equal integrated flux as source 'B', might be comprised of cold dust and gas, a short-lived tidal structure caused by the merger.

2.3 Observations

The *AKARI* IRC-NIR instrument used a filter wheel to select either one of the three imaging filters or one of the two dispersion elements. For our reference image, we used the *N*3 image filter (∼3 μm) which had a field of view of approximately 10 arcmin × 10 arcmin across 412 × 512 pixel giving a pixel scale of 1.46 arcsec. For spectroscopy, we used the grism *NG* which dispersed between 2.5–5.0 μm across 291 pixel, giving 0.0097 μm pixel^{-1}, in a 1 arcmin ×1 arcmin aperture (referred to as *Np*) which is dedicated to spectroscopy of point sources. The point spread function FWHM was 4.7 arcsec in imaging mode and ∼6.7 arcsec in spectroscopic mode.

We selected the spectroscopy Astronomical Observing Template *IRCZ4* in the configuration *b; Np* (which selects the grism and the point source aperture). In Phase III, this configuration gives a 5σ detection limit for point sources of ∼2 mJy and a line sensitivity of ∼5 × 10^{-18} W m^{-2} for each pointing. Each pointing consisted of a reference image (see Figs 2 and 3) and at least eight exposure frames for the *NG* grism, bracketed by 10 dark frames (see Onaka et al. 2009 for details). Each frame exposure was ∼70 sec, giving an integrated exposure time for each pointing of ∼9.3 min. We carried out 10 pointings per source wherever possible.

At the redshifts of the targets considered in this paper, the Hα hydrogen recombination line falls within our 2.5–5.0 μm observed wavelength range. However, Hβ was outside our range. No other emission lines were detected. We used the reference image of the larger 10 arcmin × 10 arcmin *N*3 band field which is attached to the 1 arcmin × 1 arcmin grism field, smoothed with a 5 × 5 median boxcar, to confirm the identification of our sources with images from public archives.

2.4 Data reduction pipeline

The IRC data reduction pipeline for the warm phase (Onaka et al. 2009) was originally used to analyse our data. However, we found the correction for spacecraft jitter between the ∼8 spectroscopic frames within each pointing and sky subtraction did not yield satisfactory results, so we wrote our own pipeline using Interactive Data Language (IDL) to reduce the raw spectroscopic data.

Our new pipeline includes dark subtraction, saturation masking (physical detector saturation is detected by scaled values from a short exposure and masked out), wavelength calibration and spectral response calibration using the calibration data from the IRC pipeline. We wrote our own routines to handle sky subtraction in which we fitted a sixth-order polynomial in the dispersion direction to remove a banding pattern across the frame and a second-order polynomial in the image direction. We also wrote routines

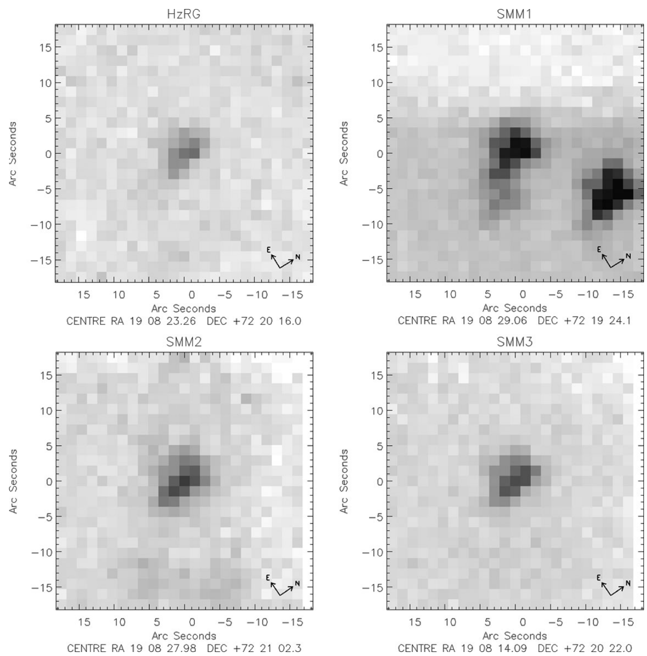

Figure 2. *AKARI* 3 μm images of the 8C1909+722 radio galaxy and its companion submillimetre galaxies. The figures are centred on the positional centroids of the sepctra and each is a median stack of the pointings taken for each source using the *N*3 filter. The dispersion direction is horizontal and the FWHM of the kernel used in the source extraction is equivalent to a width of 2 and 3 pixel in the wavelength and spatial directions, respectively.

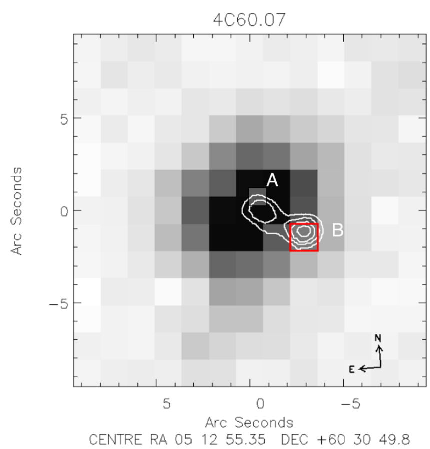

Figure 3. A blow-up of the *AKARI* 3 μm image of 4C60.07, overlaid by contours (at 3.5, 4.5, 5.5 and 6.5 σ) from the SMA 870 μm image for the centre of 4C60.07 from Ivison et al. (2008) which resolve the two submillimetre sources close to the HzRG. The labelling of the submillimetre sources 'A' and 'B' is done following Ivison et al. (2008). The radio source overlaps 'A' and is centred <0.5 arcsec north-east of it. A red square marks the positional centre of the *AKARI* spectrum. The dispersion direction is horizontal and the FWHM of the kernel used in the source extraction was equivalent to a width of 2 and 3 pixel in the wavelength and spatial directions, respectively.

to handle deglitching and to estimate the offsets between frames for each pointing caused by spacecraft jitter, using the simultaneous 10 arcmin × 10 arcmin imaging data. Our pipeline included IDL routines for zerofootprint drizzling into a grid expanded by five times in each direction and for noise-weighted feature extractions which were previously developed for the SCUBA Half Degree Extragalactic Survey (Serjeant et al. 2008), using a Gaussian with an FWHM kernel in the expanded grid of 10 and 15 pixel in the wavelength and spatial directions, respectively. This equates to an FWHM kernel of 2 and 3 pixel in the original data. We also wrote an IDL graphic user interface routine to visualize various elements of the reduction on an interactive basis. Finally, the results were stacked by coadding the noise-weighted pointings for each target. The reduced spectra had lower noise and fewer artefacts than those from the *AKARI* pipeline.

The spectroscopic flat-fields provided in the calibration data have low signal-to-noise ratio (SNR) and were found to increase the rms of our data slightly, so they were not used, following guidance in the manual (Onaka et al. 2009).

3 RESULTS

We show in Fig. 4, the spectra of the five targeted sources, four of which appear to have significant Hα emission. The spectra have been stacked by coadding the noise-weighted pointings for each source. These spectra had been smoothed in the source extraction routine during the data reduction described in Section 2.4 and were not otherwise smoothed. The SNRs of these detections are 3.1 and 2.5 for the HzRGs, and 10.0 and 2.4 for the submillimetre galaxies (see Table 2). Although some of the SNRs are relatively modest, the redshifts for the two HzRGs were already known from Lyα and other emission lines (see Section 2.2), and all four Hα line identifications were observed at the wavelengths corresponding closely to these redshifts. The estimated noise as a function of wavelength was calculated by splitting the raw data for each source into two halves and subtracting the two spectra obtained.

3.1 Spectra of the HzRGs

The spectrum for the radio galaxy 8C1909+722 HzRG has a broad Hα emission line at the correct wavelength for its redshift, as shown in Fig. 4 (top). The spectrum was taken from the centre of the target.

For the radio galaxy 4C60.07, Fig. 3 shows the *AKARI* 3 μm image overplotted with the SMA 870 μm contours from Ivison et al. (2008). There are two submillimetre peaks, the weakest (labelled 'A') coincident with the 3 μm peak and the strongest ('B') offset by about 3 arcsec. The stacked spectrum for this radio source has a broad Hα emission line at 'B' (see Fig. 4, bottom). We did not detect an Hα line at 'A'.

The FWHM of the Hα lines for the two HzRGs are shown in Table 2 and are 9400 ± 1600 and 4800 ± 1000 km s^{-1}, respectively, levels which show that dust-shrouded quasars are present in these sources.

3.2 Spectra of the submillimetre galaxies near 8C1909+722

SMM1 shows considerable structure, both in the submillimetre (see Fig. 1) and at 3 μm (see Fig. 2). The second brightest of the submillimetre peaks shows an Hα emission line, but the other peaks do not. The emission line confirms that SMM1 is at the same redshift as the radio galaxy.

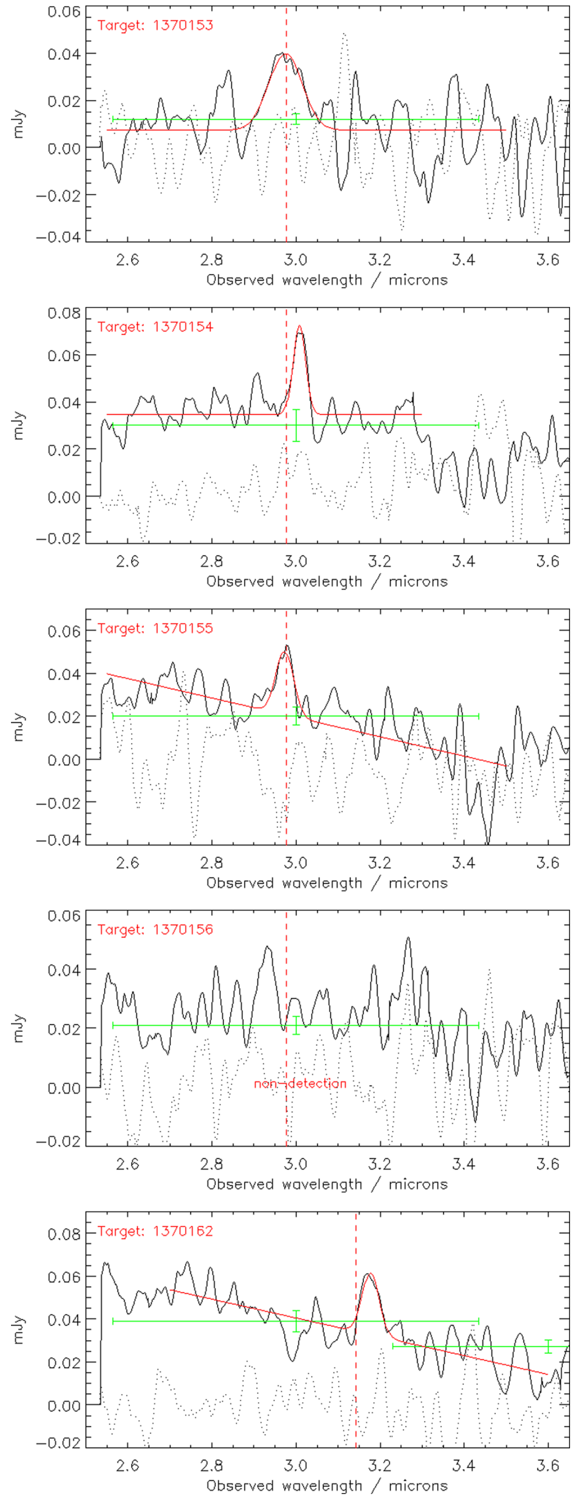

Figure 4. From top: 8C1909+722 HzRG, SMM1, SMM2, SMM3 (non-detection) and 4C60.07. The dashed red vertical lines show the position of Hα emission lines at the expected redshifts. The solid red lines show the Gaussian least-squares fits to the Hα line and continuum in the wavelength region shown. The dotted grey lines show the noise levels as a function of wavelength, calculated as described in the text. The green points at 3.0 μm are from the *AKARI* broad-band photometry (the reference image). The green point at 3.6 μm for 4C60.07 is from *Spitzer* IRAC broad-band photometry. *Spitzer* photometry for 8C1909+722 is an order of magnitude higher and may include flux from another source; 0.8 μm Keck photometry (De Breuck et al. 2001) is the same order of magnitude as the *AKARI* data.

Table 2. Estimates of SFRs and line widths. Estimates of SFR(Hα) for the SMGs are based on Hα emission luminosities and of deconvolved FWHM are based on the width of the Hα lines for the HzRGs. No adjustment for extinction has been made. FIR luminosities and SFRs are based on the 850 μm flux (see Table 1) assuming an SMMJ2135-0102 SED. SFR(Hα)s for the HzRGs are not quoted due to line contamination from their AGNs. Redshifts in italics were identified by this work.

Source	Redshift (z)	Flux(Hα) (10^{-19} W m^{-2})	SNR(Hα)	$L_{\mathrm{H}\alpha}$ (10^{36} W)	SFR$_{\mathrm{H}\alpha}$ (M$_\odot$ yr^{-1})	L_{FIR} (10^{13} L$_\odot$)	SFR$_{\mathrm{FIR}}$ (M$_\odot$ yr^{-1})	FWHM(Hα) (km s^{-1})
HzRGs								
8C1909+722 HzRG	3.536	7.9	3.1	8.6 ± 2.8	–	2.5 ± 0.2	4300 ± 1500	9400 ±1600
4C60.07 HzRG	3.788	2.8	2.5	3.6 ± 1.4	–	1.7 ± 0.3	2900 ± 1000	4800 ±1000
SMGs								
8C1909+722 SMM1	3.536	3.1	10.0	3.3 ± 0.3	260 ± 80	1.6 ± 0.2	2800 ± 1000	–
8C1909+722 SMM2	3.536	3.5	2.4	3.8 ± 1.6	300 ± 100	0.6 ± 0.2	1100 ± 500	–
8C1909+722 SMM3	–	<0.02	–	< 0.02	–	0.3 ± 0.2	500 ± 300	–

SMM2 also shows Hα emission (see Fig. 4), again at the same redshift ($z = 3.536$), confirming that this galaxy is also associated with the radio galaxy. The spectrum for SMM2 is taken from the centre of the target in the *AKARI* 3 μm image.

SMM3 does not show a peak at the expected wavelength, although there is a strong peak about 0.05 μm lower. We have not taken this as a convincing Hα emission line. Unlike SMM1 and SMM2, this galaxy is not aligned with the radio jets.

Stevens et al. (2003) suggested that the radio galaxy, the nearby submillimetre galaxies and other clumps had formed as a single galaxy cluster; we have confirmed that this association is correct in the case of two of these submillimetre sources.

3.3 Star formation rates

We have used the Hα emission lines to estimate the SFRs of the submillimetre galaxies, using the formula from Kennicutt (1998):

$$\mathrm{SFR}/(\mathrm{M}_\odot\ \mathrm{yr}^{-1}) = 7.9 \times 10^{-35} L_{\mathrm{H}\alpha}/W, \quad (1)$$

assuming a Salpeter IMF and solar abundances. The results for the two submillimetre galaxies for which we detected Hα lines are 260 ± 80 and 300 ± 100 M$_\odot$ yr^{-1}, respectively (see Table 2). No adjustment has been made for dust extinction.

We can obtain an alternative measure of the SFRs by using the 850 μm luminosity (Table 1) to estimate the 60 μm luminosity, then using the 60 μm luminosity to obtain an estimate of the far-infrared luminosity for 8–1000 μm (L_{FIR}). We have assumed the spectral energy distribution (SED) of the submillimetre galaxy SMMJ2135-0102 (the 'Eyelash') for these estimates and then used the formula for estimating the SFR from Kennicutt (1998):

$$\mathrm{SFR}/(\mathrm{M}_\odot\ \mathrm{yr}^{-1}) = 4.5 \times 10^{-37} L_{\mathrm{FIR}}/W. \quad (2)$$

The results of this calculation are shown in Table 2.

The SFRs estimated from Hα are lower than the SFRs estimated from L_{FIR} by factors of about 11 and 4, respectively, suggesting dust obscuration. Swinbank et al. (2004) found an SFR(FIR)/SFR(Hα) ratio of ∼10 in a study of submillimetre to radio galaxies in the redshift range from $z = 1.408$ to 2.692. Takata et al. (2006) found close agreement between the two methods of estimating SFRs after adjusting the Hα-based estimates for dust extinction by an average factor of 2.9 ± 0.5 in a study of submillimetre-selected ULIRGs at $0.9 < z < 2.7$. Fig. 5 shows that our SMGs have luminosities and dust extinction at comparable levels with these earlier studies.

The total FIR luminosity calculated above also shows that SMM1 and the two HzRGs are hyperluminous infrared galaxies (HyLIRGs; $L_{\mathrm{FIR}} > 10^{13}$ L$_\odot$) and SMM2 is a ULIRG.

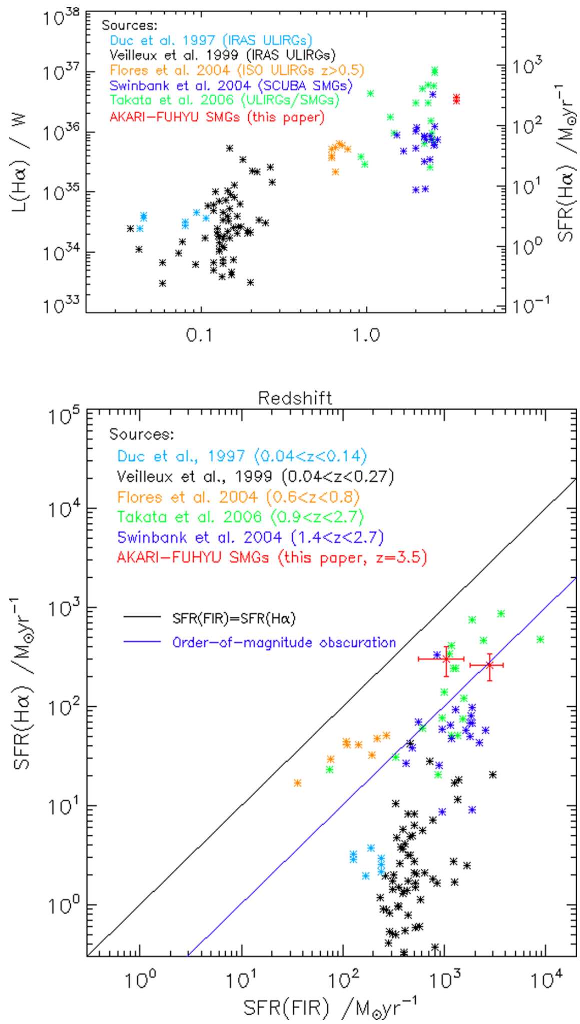

Figure 5. Top: Hα luminosity for the two SMGs as a function of redshift in comparison with earlier studies. Bottom: SFRs based on Hα luminosity versus far-infrared luminosity of the two SMGs compared to those of recent studies. Takata et al. (2006) and Flores et al. (2004) data are shown before correction for extinction. Some sources show evidence of AGNs; all are SMGs. Our results are shown in red.

4 DISCUSSION AND CONCLUSIONS

These are the first (tentative) detections of Hα emission lines in HzRGs/SMGs at $z > 2.8$.

We have found that the Hα lines in the two HzRGs are broad. Broad Hα emission lines in HzRGs are not rare (Larkin et al. 2000; Nesvadba et al. 2011) and indicate that these sources should be classified as reddened quasars rather than galaxies (see the discussion in Rawlings et al. 1995), a situation that can lead to misleading estimates of stellar populations in the host galaxy. This is a particular problem in studies using near-/mid-infrared photometry of sources which may otherwise appear to be narrow-line AGNs.

For 4C60.07, our detection of a broad Hα line was at the location of the submillimetre source 'B' (see Fig. 3). Ivison et al. (2008) suggested that 'B' was a gas-rich starburst/AGN on the basis of the red mid-infrared colours. Our discovery that 'B' is a quasar supports the argument that binary AGNs at close separations may be due to the triggering or enhancement of AGN activity during mergers. The unexpectedly high prevalence of binary quasars at high redshifts (Djorgovski 1991; Hennawi et al. 2010) provided strong support for this idea. A recent study of binary quasars found that simple halo occupation distribution models underpredict quasar clustering at small separations (Kayo & Oguri 2012). That such a well-studied source had not previously been shown to be a quasar adds to the evidence that there is a higher fraction of binary AGN/quasars at high redshift than previously realized.

Our Hα luminosity and FWHM results for the two HzRGs are both consistent with those of lower redshift radio galaxies (e.g. Nesvadba et al. 2011).

Our detection of Hα emission lines from two submillimetre galaxies in the region of 8C1909+722 provides confirmation of their association with the HzRG. The extent of the system is ∼700 kpc (based on Stevens et al. 2003), suggesting that this may be evolving into a cluster of galaxies or possibly a single galaxy. The complex SMM1 is ∼80 kpc in extent and appears to be in the process of merging. In the 8C1909 field, we have the first confirmation of multiple U/HyLIRGs in a protocluster region at $z > 3$, giving a combined SFR of $\sim 8000\,M_{\odot}\,yr^{-1}$.

The high levels of star formation in the two SMGs are shown with previous results in Fig. 5. Our Hα luminosities and SFR(FIR)/SFR(Hα) ratios are comparable to those found in recent studies at $0.9 < z < 2.7$ suggesting similar levels of dust obscuration.

ACKNOWLEDGEMENTS

This research is based on observations with *AKARI*, a JAXA project with participation of ESA. This work was supported by STFC under grant ST/G002533/1. IRS acknowledges support from STFC and the Leverhulme Trust. MI acknowledges support from the Creative Research Initiative programme no. 2010-0000712 of NRFK. Thanks to Mark Swinbank for the SMMJ2135-0102 SED. Thanks also to the anonymous referee for many helpful comments.

REFERENCES

Alexander D. M., Smail I., Bauer F. E., Chapman S. C., Blain A. W., Brandt W. N., Ivison R. J., 2005, Nat, 434, 740
Barger A. J., Cowie L. L., Sanders D. B., Fulton E., Taniguchi Y., Sato Y., Kawara K., Okuda H., 1998, Nat, 394, 248
Bower R. G., Benson A. J., Malbon R., Helly J. C., Frenk C. S., Baugh C. M., Cole S., Lacey C. G., 2006, MNRAS, 370, 645
Boyle B. J., Terlevich R. J., 1998, MNRAS, 293, L49
Calzetti D., Armus L., Bohlin R. C., Kinney A. L., Koornneef J., Storchi-Bergmann T., 2000, ApJ, 533, 682
Chapman S. C., Blain A. W., Smail I., Ivison R. J., 2005, ApJ, 622, 772
Croton D. J. et al., 2006, MNRAS, 365, 11
De Breuck C. et al., 2001, AJ, 121, 1241
di Matteo T., Springel V., Hernquist L., 2005, Nat, 433, 604
Djorgovski S., 1991, in Crampton D., ed., ASP Conf. Ser. Vol. 21, The Space Distribution of Quasars. Astron Soc. Pac., San Francisco, p. 349
Duc P. A., Mirabel I. F., Maza J., 1997, A&AS, 124, 533
Ferrarese L., Merritt D., 2000, ApJ, 539, L9
Flores H., Hammer F., Elbaz D., Cesarsky C. J., Liang Y. C., Fadda D., Gruel N., 2004, A&A, 415, 885
Franceschini A., Hasinger G., Miyaji T., Malquori D., 1999, MNRAS, 310, L5
Gebhardt K. et al., 2000, ApJ, 539, L13
Genzel R. et al., 1998, ApJ, 498, 579
Greve T. R., Ivison R. J., Papadopoulos P. P., 2004, A&A, 419, 99
Greve T. R., Ivison R. J., Stevens J. A., 2006, Astron. Nachr., 327, 208
Harrison C. M. et al., 2012, , ApJ, 760, L15
Hennawi J. F. et al., 2010, ApJ, 719, 1672
Hughes D. H. et al., 1998, Nat, 394, 241
Ivison R. J. et al., 2008, MNRAS, 390, 1117
Ivison R. J. et al., 2012, MNRAS,, 425, 1320
Kayo I., Oguri M., 2012, , MNRAS, 424, 1363
Kennicutt R. C., Jr, 1998, ARA&A, 36, 189
Larkin J. E. et al., 2000, ApJ, 533, L61
Magorrian J. et al., 1998, AJ, 115, 2285
Murakami H. et al., 2007, PASJ, 59, S369
Nesvadba N. P. H., De Breuck C., Lehnert M. D., Best P. N., Binette L., Proga D., 2011, A&A, 525, A43
Onaka T. et al., 2007, PASJ, 59, S401
Onaka T., Lorente R., Ita Y., Ohyama Y., Tanabe T., Pearson C., 2009, AKARI IRC Data User Manual. JAXA/ISAS, Japan
Papadopoulos P. P., Röttgering H. J. A., van der Werf P. P., Guilloteau S., Omont A., van Breugel W. J. M., Tilanus R. P. J., 2000, ApJ, 528, 626
Pearson C. P. et al., 2010, A&A, 514, A9
Rawlings S., Lacy M., Sivia D. S., Eales S. A., 1995, MNRAS, 274, 428
Roettgering H. J. A., van Ojik R., Miley G. K., Chambers K. C., van Breugel W. J. M., de Koff S., 1997, A&A, 326, 505
Serjeant S. et al., 2008, MNRAS, 386, 1907
Smail I., Ivison R. J., Blain A. W., 1997, ApJ, 490, L5
Spoon H. W. W., Marshall J. A., Houck J. R., Elitzur M., Hao L., Armus L., Brandl B. R., Charmandaris V., 2007, ApJ, 654, L49
Springel V., Di Matteo T., Hernquist L., 2005, MNRAS, 361, 776
Stevens J. A. et al., 2003, Nat, 425, 264
Swinbank A. M., Smail I., Chapman S. C., Blain A. W., Ivison R. J., Keel W. C., 2004, ApJ, 617, 64
Takata T., Sekiguchi K., Smail I., Chapman S. C., Geach J. E., Swinbank A. M., Blain A., Ivison R. J., 2006, ApJ, 651, 713
Veilleux S., Kim D. C., Sanders D. B., 1999, ApJ, 522, 113

This paper has been typeset from a TEX/LATEX file prepared by the author.